Sensors & Diagnostics

PAPER

View Article Online
View Journal | View Issue

Cite this: *Sens. Diagn.*, 2024, **3**, 1672

Competitive horseradish peroxidase-linked aptamer assay for sensitive detection of 17β-estradiol with a new aptamer†

Qiuyi Cheng[ab] and Qiang Zhao *[abc]

17β-Estradiol (E2) is one of the typical endocrine-disrupting compounds (EDCs), which plays a major role in facilitating the growth and regulating the balance of the human endocrine system. E2 contamination can cause environmental and health risks as E2 exposure can interfere with the endocrine system by binding to estrogen receptors. It is imperative to develop sensitive methods for E2 detection. Herein we developed a competitive enzyme-linked aptamer assay for E2 detection by using a newly reported high-affinity DNA aptamer as an affinity ligand. The complementary DNA (cDNA) of the anti-E2 aptamer is conjugated on a microplate. Horseradish peroxidase (HRP) is labeled on the aptamer probe. In the absence of E2, HRP-labeled aptamer is captured by cDNA, and HRP catalyzes the substrate into a product, generating an absorbance signal or chemiluminescence signal. In the presence of E2, E2 binds with the aptamer, causing displacement of HRP-labeled aptamer from the microplate and a decrease in signals. In absorbance-analysis mode, the detection limit of E2 reached 0.2 nmol L^{-1} with a dynamic range from 0.2 nmol L^{-1} to 20 μmol L^{-1}. In chemiluminescenceanalysis mode, this method enabled the quantification of E2 at 50 pmol L^{-1}, with a dynamic range from 50 pmol L^{-1} to 50 μmol L^{-1}. This method could also detect E2 spiked in lake water samples, showing promise in practical applications.

Received 22nd June 2024,
Accepted 5th August 2024

DOI: 10.1039/d4sd00208c

rsc.li/sensors

Introduction

17β-Estradiol (E2) is the most typical steroid hormone secreted by gonads, which is in control of the growth and sexual maturity of animals.[1] The overuse of E2 in medicine and livestock farming, causing large amounts of endocrine-disrupting chemicals (EDCs) to be released into the environmental medium, is a common issue of great concern.[2] The residual E2 in the environment is often bioaccumulated and concentrated in the human body through the food chain, mimicking the behavior of female sex hormones and combining with the estrogen receptors.[3–6] It may influence the capacity of the reproductive system and break the balance of hormone metabolism in the human body, even at a trace level (ng L^{-1}).[7] Chronic E2 exposure might cause a series of diseases, such as endocrine disorders, reproductive dysfunction, and infertility.[8] Therefore, to guarantee human health and food safety, there is an urgent requirement for sensitive detection of E2.[9–13] Nowadays, the traditional method for E2 detection is HPLC-MS analysis, which exhibits high accuracy and sensitivity.[10,11] However, it suffers from the need for expensive instruments and requires trained and qualified personnel, a time-consuming pre-treatment process, and environment-hazardous organic reagents as the mobile phase. Immunoassay is another method for E2 detection.[12,13] The application of immunoassay has some limitations in antibody preparation with high cost, poor stability of antibody and batch-to-batch variation of antibody.[14]

The aptamer is a short single-stranded oligonucleotide, which specifically recognizes target molecules with high affinity, and the target can be metal ions, small molecules and proteins.[15–17] Aptamers can be obtained *in vitro* by the SELEX (systematic evolution of ligands by exponential enrichment) technique. Aptamers possess some remarkable merits, such as low cost, facile synthesis, easy modification and high stability. Aptamers are promising in developing biosensors. Up to now, a few anti-E2 aptamers have been selected.[18] In recent years, aptamer-based assays for E2 with versatile formats have been developed.[18–20] Kim *et al.* reported a fluorescence method, through a target-triggered conformational change of the fluorophore and quencher-labelled aptamer probe linked with its complementary sequence.[19] Liu *et al.* constructed an electrochemical label-free aptasensor using

[a] *State Key Laboratory of Environmental Chemistry and Ecotoxicology, Research Center for Eco-Environmental Sciences, Chinese Academy of Sciences, Beijing, 100085, China. E-mail: qiangzhao@rcees.ac.cn*
[b] *University of Chinese Academy of Sciences, Beijing, 100049, China*
[c] *School of Environment, Hangzhou Institute for Advanced Study, UCAS, Hangzhou 310024, China*

† Electronic supplementary information (ESI) available. See DOI: https://doi.org/10.1039/d4sd00208c

graphene to mediate the electron transfer.[20] Pu *et al.* developed a colorimetric assay, based on target binding-induced aggregation of gold nanoparticles to generate visible colour change.[21] However, the E2-aptamers selected in the past have too long sequences or show poor affinities.[22] Recently, Liu and coworkers successfully selected a new aptamer named CN-Es2 (5′-CGA CTT AAG GTA TGT GAT CTT AGT TGT AGT TCA AGT CG-3′) with a short sequence and high-binding affinity.[22]

ELISA (enzyme-linked immunosorbent assay) is a common method for sensitive and rapid detection of targets. The replacement of antibodies with aptamers in ELISA has aroused wide interest in constructing analysis methods, overcoming the limitations of antibodies.[23,24] A few competitive enzyme-linked aptamer assays (ELAAs) are reported for E2 detection.[25–29] Long *et al.* described a fibre optic chemiluminescent aptasensor,[25] and an E2-ovalbumin conjugate was attached to the optical fibre for an indirect competitive assay. Skouridou *et al.* built a microtiter plate-based assay,[26] in which a chemical derivative of E2 was immobilized on activated plate wells to capture enzyme-conjugated aptamer probes for signal amplification. However, the reported ELAAs have some shortcomings, such as sophisticated surface modification processes, troublesome experimental steps and indispensable chemical modification of E2.

In this work, we developed a competitive enzyme-linked aptamer assay based on the newly reported high-affinity E2-aptamer sequence (CN-Es2). In this strategy, the biotinylated complementary strand (cDNA) of the aptamer CN-Es2 is modified on streptavidin (SA)-coated microplate through the specific strong interaction between SA and biotin. SA-conjugated horseradish peroxidase HRP (termed HRP-SA) is linked to a biotin-labeled aptamer to construct the HRP-aptamer probe for target recognition and signal amplification. In the absence of E2, the HRP-aptamer probe hybridizes with the cDNA on the microplate surface. The anchored HRP catalyses the substrates into products, generating absorbance or chemiluminescence signals. When E2 exists, HRP-aptamer binds with E2 instead of the cDNA, causing a reduction of the amount of HRP-aptamer probe on the microplates and a signal decrease. E2 is detected by measuring the signal change. This method was able to selectively detect E2, and it was also capable of detecting E2 spiked in lake water samples.

Experimental

Reagents and materials

17β-Estradiol (E2), bisphenol A (BPA), adenosine triphosphate (ATP), L-histidine (L-His), L-arginine (L-Arg), L-tyrosine (L-Tyr), kanamycin (KANA), tetracycline (TC), streptavidin (SA), bovine serum albumin (BSA), horseradish peroxidase-conjugated streptavidin (HRP-SA) and femto-ELISA-HRP substrates (3,3′,5,5′-tetramethylbenzidine dihydrochloride, TMB) were purchased from Sangon Biotech (Shanghai, China). All the DNA oligonucleotides (Table S1 in the (ESI†)), which had one biotin label at 3′-end and a tetraethylene glycol (TEG) linker, were synthesized and purified by Sangon Biotech Co., Ltd. (Shanghai, China). The chemiluminescent-substrate solution of HRP was obtained from Sigma-Aldrich (USA). All solutions were prepared with ultrapure water obtained from an Elga Labwater System (Purelab Ultra Genetic, England). Lake water was obtained from Beijing Olympic Forest Park (Beijing, China).

Characterizing the affinity of aptamer to E2

Isothermal titration calorimetry (ITC) was performed using MicroCal PEAQ-ITC (Malvern Panalytical Ltd). At 25 °C, 280 μL of 5 μM unlabelled aptamer CN-Es2 in binding buffer (20 mM Tris-HCl (pH 7.5), 10 mM $MgCl_2$, 100 mM NaCl) was filled in the sample cell. 60 μL of 100 μM E2 solution in the same buffer was loaded into the syringe. In the beginning, 0.4 μL of E2 was titrated into the sample cell, and then 2.0 μL of E2 was titrated every 100 seconds for 19 times. During titration, the stirring speed of the syringe was chosen as 750 rpm, and the reference power was set at 10.0 μcal s^{-1}. By integrating the area under the peaks in the injection plot, the heat change was used to fit a titration curve to a one-set binding model with the MicroCal PEAQ-ITC analysis software for the calculation of dissociation constant (K_d).

Preparation of complementary DNA-coated microplate

At first, 100 μL of the coating buffer (Table S2†) was added into the wells of high-binding 96-well clear microplate (Corning) for the absorbance assay or high-binding 96-well black microplate (NUNC Maxisorp plates offered by Thermo Scientific (USA)) for chemiluminescence assay and incubated for 12 h at 4 °C to prepare a streptavidin (SA)-coated microplate. The wells were washed three times with 200 μL of washing buffer (Table S2†), and 200 μL of blocking buffer (Table S2†) was added to the wells. Then, the wells were blocked after incubating for 1 hour at room temperature under shaking. After washing with 300 μL of washing buffer, 100 μL of 20 nM biotinylated complementary DNA (cDNA) in the immobilization buffer (Table S2†) was added into the SA-coated well, and incubated under shaking for 1 hour at room temperature. Finally, the wells were washed three times with 200 μL of assay buffer (Table S2†), and the complementary DNA-coated microplate was obtained.

Detection of E2

The biotinylated E2 aptamer (denoted as Es2-Apt) and SA-conjugated HRP were incubated in the assay buffer at 4 °C for 30 min (1 : 1) to obtain the HRP-labeled aptamer probe (3 nM). Next, a certain concentration of E2 was incubated at 4 °C for 10 min with the HRP-labeled aptamer probe to form the E2-aptamer complex. The mixture was added into the cDNA-coated wells and incubated for 15 min at 4 °C. After that, the microplate was washed three times with 200 μL of assay buffer. Then, 100 μL of the substrate solution (TMB or

chemiluminescent-substrate) was added into the wells. In absorbance-analysis mode, 100 μL of 1 M HCl was added to stop the reaction after a 10 min incubation at room temperature, and then the absorbance signal was recorded at a wavelength of 450 nm by a Synergy H1 microplate reader (BioTek, USA). In chemiluminescence mode, after an 8 min incubation of the chemiluminescent-substrate solution at room temperature, the chemiluminescence signal was measured using the microplate reader. Duplicate samples were tested. Each sample was measured three times, and the average value was used for data processing.

In the selectivity test, some non-target substances, including L-histindine, L-arginine, L-tyrosine, kanamycin, tetracycline, ATP and bisphenol A, were tested. All of these non-target substances and E2 were tested at 100 nM. All other experiment conditions were the same as described above in the competitive enzyme-linked aptamer assay for E2.

Detection of E2 in complex sample matrix

Lake water was diluted 50-fold with the assay buffer and used as a complex sample matrix. Before diluting, the lake water was centrifuged at 12 000 rpm for 15 min, and then the supernatant was filtered using a 0.22 μm membrane. E2 spiked in the diluted lake water was tested by the enzyme-linked aptamer assay described above.

Results and discussion

Principle of assay

Fig. 1 shows the schematic of a competitive enzyme-linked aptamer assay for E2 detection. The biotinylated complementary DNA (cDNA) of aptamer CN-Es2 was immobilized on the SA-coated wells to obtain a cDNA-coated microplate. The HRP-labeled aptamer probe was added to this cDNA-coated well. In the absence of E2, HRP-labeled aptamer was captured by the cDNA. HRP converts the substrate into the product, generating an absorbance signal or chemiluminescence signal. In the presence of E2, the aptamer probe prefers to bind with the target, not hybridizing with the cDNA on the microplate, which causes a decrease of HRP-labeled aptamer on the microplate. Finally, E2 is detected by measuring signal change through absorbance or chemiluminescence-analysis.

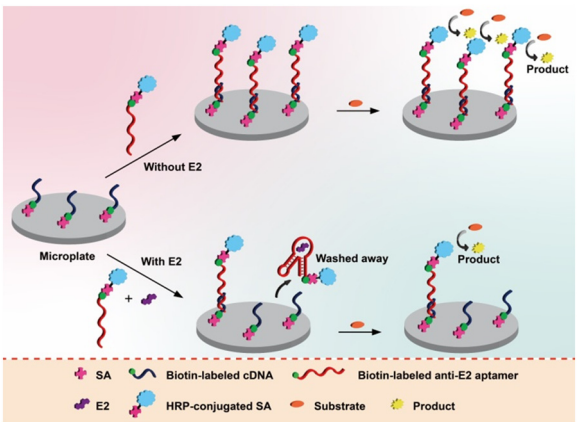

Fig. 1 The schematic of competitive enzyme-linked aptamer assay for E2 detection.

Feasibility of assay

We chose to use a newly reported anti-E2 aptamer CN-Es2 as an affinity ligand in our assay. Isothermal titration calorimetry (ITC) measurement was conducted to verify the affinity of aptamer CN-Es2. As shown in Fig. S1,† the ITC result indicated the aptamer had a high-affinity with a dissociation constant (K_d) at 55.3 nM (Table S3†), which is close to that from a previous report.[22]

We first tested the feasibility of a competitive enzyme-linked aptamer assay for E2 detection with absorbance-analysis by using a cDNA C16-modified microplate (Table S1†). As illustrated by the absorbance-analysis mode (Fig. 2), in the absence of E2, the existence of an HRP-labeled aptamer probe gave rise to a significant signal increase, indicating that the aptamer could be successfully captured by cDNA. In the presence of E2, the absorbance signal decreased obviously. This phenomenon was caused by the affinity binding between the aptamer and E2, which led to the reduction of aptamer on the surface of the microplate. The result demonstrates that the proposed assay is feasible for the detection of E2.

Optimization of experimental conditions

The length of the complementary DNA (cDNA) is a key factor in the assay performance. It determined the combination stability between aptamer and cDNA, influencing the response signal strength. Thus, we first optimized the length of cDNA with 12, 14 and 16 nucleotides (denoted as C12, C14

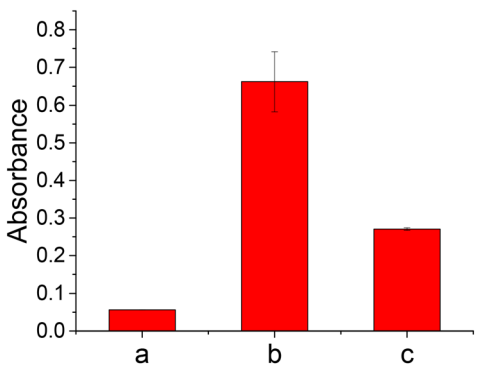

Fig. 2 Feasibility test of the competitive enzyme-linked aptamer assay for E2 detection. (a) Absorbance signal of the sample without HRP-labeled aptamer probe. (b) Absorbance signal of the blank sample without E2. (c) Absorbance signal of the E2 sample (100 nM). The cDNA C16 (20 nM) in the immobilization buffer was used to coat the microplate. The concentration of HRP-labeled aptamer was 1 nM. The assay buffer contained 20 mM Tris-HCl (pH 7.5), 10 mM $MgCl_2$ and 100 mM NaCl. The immobilized cDNA and E2-aptamer complex were incubated at 4 °C for 15 min.

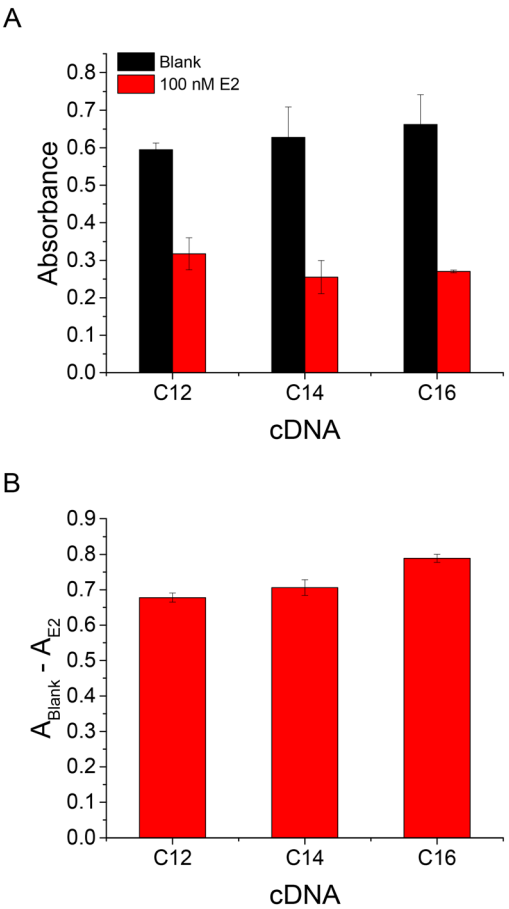

Fig. 3 (A) Effect of cDNA length on the blank signal and the signal of the sample solution containing 100 nM E2. (B) Effect of cDNA length on the absorbance change caused by 100 nM E2 (obtained by subtracting the absorbance signal of the blank sample from the absorbance signal of the E2 sample). 1 nM HRP-labeled aptamer was applied. 20 nM cDNA was used in immobilization buffer for preparation of cDNA-coated microplate. The immobilized cDNA and E2-aptamer complex were incubated at 4 °C for 15 min.

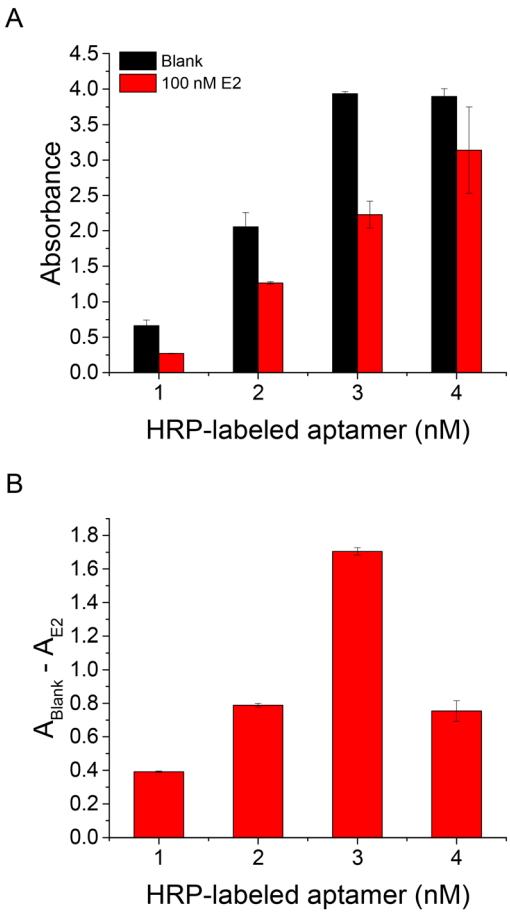

Fig. 4 (A) Effect of HRP-labeled aptamer concentration on the blank signal and the signal of the sample solution containing 100 nM E2. (B) Effect of HRP-labeled aptamer concentration on the absorbance change caused by 100 nM E2 (obtained by subtracting the absorbance signal of the blank sample from the absorbance signal of the E2 sample). 20 nM cDNA C16 was used for the preparation of cDNA-coated microplate. The immobilized cDNA and E2-aptamer complex were incubated at 4 °C for 15 min.

and C16, respectively). As depicted in Fig. 3A, when the longer cDNA was used, the higher blank signal was produced, meaning the hybridization between aptamer and immobilized cDNA was strengthened. A_{Blank} indicated the absorbance signal of the blank sample, and A_{E2} represented the absorbance signal of the sample solution containing 100 nM E2. The maximal difference between A_{E2} and A_{Blank} was observed when the conjugated cDNA contained 16 nucleotides (Fig. 3B). Therefore, we chose C16 as the capture strand.

The concentration of HRP-labeled aptamer is another factor, that affects the amount of the captured probe on a microplate. The increase of HRP-labeled aptamer resulted in the rise of blank signal (Fig. 4A), and the decrease of absorbance signal caused by E2 (calculated by $(A_{Blank}–A_{E2})$) reached the maximum until the concentration of HRP-labeled aptamer was 3 nM (Fig. 4B). It can be explained that the addition of larger amount of HRP-labeled aptamer to the competition system may result in more HRP being left on the microplate to produce a higher response signal. However, when excessive aptamer existed in the system, E2 was captured by the excessive aptamer directly and did not participate in the competition process, causing a weakened sensitivity. Thus, we chose to use 3 nM HRP-labeled aptamer in the assay.

To obtain high sensitivity, the effect of the amount of cDNA on the microplate was also investigated. As exhibited in Fig. S2A,† a blank signal was enhanced with the increase of cDNA and finally reached a plateau. It demonstrated that the amount of cDNA on the microplate reached saturation until its concentration was up to 5 nM. Fig. S2B† shows the absorbance signal change caused by 100 nM E2 with different concentrations of the used cDNA. The decrease of the absorbance signal caused by E2 gradually increased with the increase of cDNA and a relatively larger signal change was obtained when 20 nM cDNA was applied for the preparation of the cDNA-coated microplate. Therefore, 20 nM cDNA was used to prepare a cDNA-coated microplate.

The effect of magnesium ion concentration in the assay buffer was investigated. Mg^{2+} can facilitate the hybridization between cDNA and aptamer and improve the affinity of aptamer to E2. Therefore, the balance of the competitive reaction was regulated by the Mg^{2+} concentration. As shown in Fig. 5A, the blank signal gradually increased with the increase of Mg^{2+}. This phenomenon can be interpreted as the capture process of the HRP-labeled aptamer by the immobilized cDNA was promoted. The change in the absorbance signal caused by E2 also grew with the increase of Mg^{2+} concentration, and a maximum value was obtained at 10 mM Mg^{2+} (Fig. 5B). Thus, 10 mM Mg^{2+} was used for E2 competition. Furthermore, the effect of sodium concentration in the assay buffer was investigated (Fig. S3†). Na^{+} in the assay buffer was able to enhance the signal change caused by E2, and 150 mM Na^{+} was adopted in the assay buffer.

The incubation temperature and incubation time in the competition process were also optimized. With the increase in the incubation temperature, the blank signal increased gradually and the change of the absorbance signal caused by E2 decreased (Fig. S4†). It indicated that higher temperature could unfold the hairpin structure of the aptamer, which was formed spontaneously, and thus the higher incubation temperature facilitated the formation of a duplex between cDNA and aptamer. Meanwhile, the affinity of the aptamer became weak. With the extension of the incubation time, the blank signals increased (Fig. S5†). It suggested that the longer incubation time was favourable for the formation of the duplex, but it was unfavourable for the competition induced by the target. According to the change of the absorbance signal before and after the addition of E2, incubation at 4 °C for 15 min was adopted for the E2 detection.

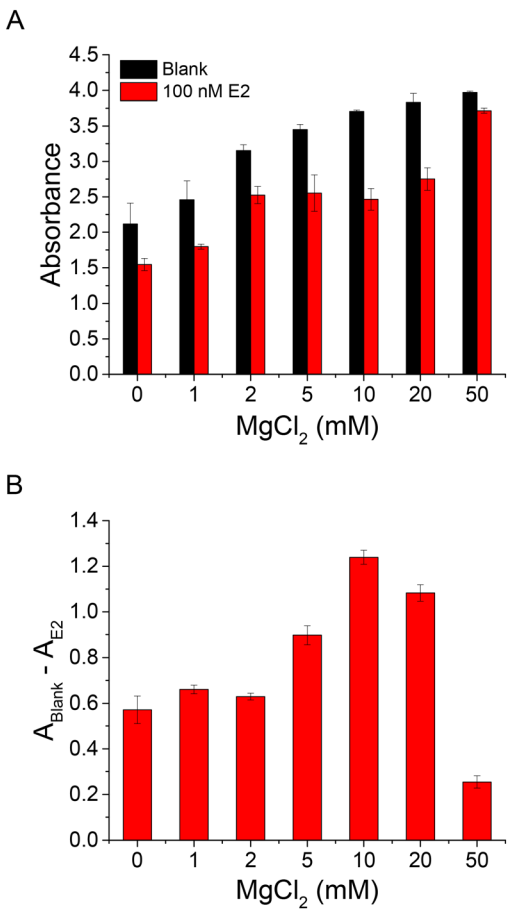

Fig. 5 (A) Effect of $MgCl_2$ concentration on absorbance signals in the absence or in the presence of 100 nM E2. (B) Effect of $MgCl_2$ concentration on the decrease of absorbance signal caused by 100 nM E2 (obtained by subtracting the absorbance signal of blank sample from the absorbance signal of E2 sample). 3 nM HRP-labeled aptamer was applied. 20 nM cDNA was used in the immobilization buffer for the preparation of the cDNA-coated microplate. The assay buffer contained 20 mM Tris-HCl (pH 7.5), 100 mM NaCl, and varying concentrations of $MgCl_2$.

Competitive enzyme-linked aptamer assay for E2 detection

Under optimal conditions, this proposed assay successfully achieved the detection of E2 with the absorbance-analysis mode. The signal gradually decreased with the increase of E2 concentrations (Fig. 6). The detection limit was 0.2 nM (~0.006 μg L^{-1}, which determined that the signal change caused by E2 was three times that of the standard deviation of blank samples). The dynamic range was from 0.2 nM to 20 μM, and the linear range was from 0.2 nM to 200 nM ($y = -0.660 \lg x + 2.42$, $R^2 = 0.998$, where y is the absorbance signal, and x is the concentration of E2). When a chemiluminescence substrate was applied, the detection limit was further lowered to 50 pM (~0.001 μg L^{-1}) by using the chemiluminescence-analysis mode (Fig. S6†), and the dynamic range was from 50 pM to 50 μM, and the linear range was from 50 pM to 50 nM ($y = -44171.7 \lg x + 151545.1$, $R^2 = 0.996$, where y is the chemiluminescence signal, and x is the concentration of E2). The detection limit was comparable to some of the reported methods for E2 detection (Table S4†).[22,25,27,29–40] The detection limits (LODs) of our assays

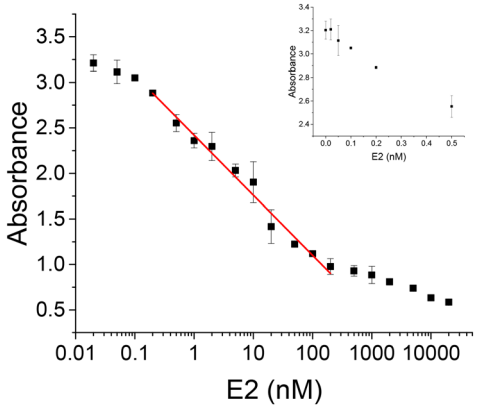

Fig. 6 Detection of E2 by ELAA with absorbance-analysis mode at optimal conditions. The inset shows the absorbance signals corresponding to blank samples and low concentrations of E2. The assay buffer contained 20 mM Tris-HCl (pH 7.5), 10 mM $MgCl_2$, 150 mM NaCl.

reached the regulatory requirements proposed by the United States Food and Drug Administration (0.12 μg L^{-1}) and the European Union (0.05 μg L^{-1}).[25]

Selectivity test and detection of E2 in complex sample matrix

The constructed assay was challenged with some non-target substances, involving L-histidine (L-His), L-arginine (L-Arg), L-tyrosine (L-Tyr), kanamycin (KANA), tetracycline (TC), adenosine triphosphate (ATP) and bisphenol A (BPA) at the concentration of 100 nM. These non-target substances did not cause significant signal changes. Furthermore, the coexistence of these non-target substances with E2 did not interfere with the response of E2 (Fig. S7†). The results show the assay is selective for E2 detection.

To confirm the ability of this ELAA for E2 detection in real environmental water samples, we tested the spiked E2 in 50-fold diluted lake water. In a complex sample matrix, this method allowed the detection of E2 in the range from 0.2 nM to 20 000 nM with the absorbance-analysis mode (Fig. S8A†), or in the range from 0.05 nM to 50 000 nM with the chemiluminescence-analysis mode (Fig. S8B†). These results indicate that the proposed assay can be used for E2 detection in a complex sample matrix.

Conclusions

We developed a competitive enzyme-linked aptamer assay for 17β-estradiol detection using the newly selected high-affinity aptamer. This method took full advantage of the aptamer, such as easy synthesis, high-affinity, facile labelling and the unique feature of aptamer that the combination of aptamer and target molecule is competitive with the hybridization of aptamer and cDNA. The use of an absorbance substrate allowed the detection of E2 with a LOD of 0.2 nM. The detection limit was further reduced to 50 pM with the use of a chemiluminescence substrate. This method enabled the detection of E2 in the complex sample matrix. In our strategy, the complementary strand was immobilized on the microplate, and the complicated covalent conjugating process of the target molecule on the microplate was avoided. This work is promising for the detection of E2 in real samples.

Data availability

The authors confirm that the data supporting the findings of this study are available within the article [and/or its ESI†].

Conflicts of interest

There are no conflicts to declare.

Acknowledgements

We thank the financial support from the National Natural Science Foundation of China (22074156) and the Strategic Priority Research Program of the Chinese Academy of Sciences (XDB0750100).

Notes and references

1 D. deCatanzaro, *Horm. Behav.*, 2015, **68**, 103–116.
2 M. Adeel, X. Song, Y. Wang, D. Francis and Y. Yang, *Environ. Int.*, 2017, **99**, 107–119.
3 T. Hintemann, C. Schneider, H. F. Schoeler and R. J. Schneider, *Water Res.*, 2006, **40**, 2287–2294.
4 H. Pu, Z. Huang, D.-W. Sun and H. Fu, *Crit. Rev. Food Sci. Nutr.*, 2019, **59**, 2144–2157.
5 M. Soeffker and C. R. Tyler, *Crit. Rev. Toxicol.*, 2012, **42**, 653–668.
6 S. Rajabi, S. Saberi, H. Najafipour, M. Askaripour, M. A. Rajizadeh, S. Shahraki and S. Kazeminia, *Mol. Biol. Rep.*, 2024, **51**, 137.
7 E. J. Routledge, D. Sheahan, C. Desbrow, G. C. Brighty, M. Waldock and J. P. Sumpter, *Environ. Sci. Technol.*, 1998, **32**, 1559–1565.
8 Q. Wei, P. Zhang, H. Pu and D.-W. Sun, *Food Chem.*, 2022, **373**, 131591.
9 Y. Guo, Z. Han, H. Min, Z. Chen, T. Sun, L. Wang, W. Shi and P. Cheng, *Small Struct.*, 2022, **3**, 2100113.
10 Y. Yang, Y. Sun, H. Chen, X. Dang, Y. Ai, X. Liu and H. Chen, *Anal. Methods*, 2020, **12**, 507–513.
11 Y. Shi, D. D. Peng, C. H. Shi, X. Zhang, Y. T. Xie and B. Lu, *Food Chem.*, 2011, **126**, 1916–1925.
12 J. Leivo, L. Kivimaki, E. Juntunen, K. Pettersson and U. Lamminmaki, *Anal. Bioanal. Chem.*, 2019, **411**, 5633–5639.
13 Y. Toishi, N. Tsunoda, K. Kume, K. Nagaoka, G. Watanabe and K. Taya, *J. Reprod. Dev.*, 2016, **62**, 631–634.
14 Z. M. Cao, T. A. Swift, C. A. West, T. G. Rosano and R. Rej, *Clin. Chem.*, 2004, **50**, 160–165.
15 E. M. McConnell, I. Cozma, D. Morrison and Y. F. Li, *Anal. Chem.*, 2020, **92**, 327–344.
16 W. Zhou, P. J. Huang, J. Ding and J. Liu, *Analyst*, 2014, **139**, 2627–2640.
17 F. Li, H. Q. Zhang, Z. X. Wang, A. M. Newbigging, M. S. Reid, X. F. Li and X. C. Le, *Anal. Chem.*, 2015, **87**, 274–292.
18 M. Svobodova, V. Skouridou, M. Luz Botero, M. Jauset-Rubio, T. Schubert, A. S. Bashammakh, M. S. El-Shahawi, A. O. Alyoubi and C. K. O'Sullivan, *J. Steroid Biochem. Mol. Biol.*, 2017, **167**, 14–22.
19 J.-Y. Kim, J.-H. Park, M. I. Kim, H. H. Lee, H. L. Kim, K.-S. Jeong, S.-O. Moon, P.-W. Kang, K.-W. Park, Y.-H. Lee and B.-W. Chun, *Int. J. Leg. Med.*, 2018, **132**, 91–98.
20 M. Liu, H. Ke, C. Sun, G. Wang, Y. Wang and G. Zhao, *Talanta*, 2019, **194**, 266–272.
21 H. Pu, Z. Huang, D.-W. Sun, X. Xie and W. Zhou, *Water, Air, Soil Pollut.*, 2019, **230**, 124.
22 C. Niu, C. Zhang and J. Liu, *Environ. Sci. Technol.*, 2022, **56**, 17702–17711.
23 L. Barthelmebs, J. Jonca, A. Hayat, B. Prieto-Simon and J. L. Marty, *Food Control*, 2011, **22**, 737–743.
24 L. Sun and Q. Zhao, *Talanta*, 2018, **179**, 344–349.

25 R. Yang, J. Liu, D. Song, A. Zhu, W. Xu, H. Wang and F. Long, *Microchim. Acta*, 2019, **186**, 726.
26 M. Jauset-Rubio, M. Luz Botero, V. Skouridou, G. Betul Aktas, M. Svobodova, A. S. Bashammakh, M. S. El-Shahawi, A. O. Alyoubi and C. K. O'Sullivan, *ACS Omega*, 2019, **4**, 20188–20196.
27 H. Yang and D. Xu, *Talanta*, 2022, **240**, 123094.
28 J.-H. Zhu, M. Wang, L.-H. Tu, A.-J. Wang, X. Luo, L.-P. Mei, T. Zhao and J.-J. Feng, *Sens. Actuators, B*, 2021, **347**, 130553.
29 L.-H. Tu, J.-H. Zhu, A.-p. Tanjung, M. Wang, J. Kang, A.-J. Wang, L.-P. Mei, Y. Xue and P. Song, *Microchim. Acta*, 2022, **189**, 56.
30 Q. Li, X. Li, P. Zhou, R. Chen, R. Xiao and Y. Pang, *Biosens. Bioelectron.*, 2022, **215**, 114548.
31 Y. Wang, X. Zhao, M. Zhang, X. Sun, J. Bai, Y. Peng, S. Li, D. Han, S. Ren, J. Wang, T. Han, Y. Gao, B. Ning and Z. Gao, *Anal. Chim. Acta*, 2020, **1116**, 1–8.
32 G. Zhang, T. Li, J. Zhang and A. Chen, *Sens. Actuators, B*, 2018, **273**, 1648–1653.
33 J.-J. Zhang, J.-T. Cao, G.-F. Shi, K.-J. Huang, Y.-M. Liu and Y.-H. Chen, *Anal. Methods*, 2014, **6**, 6796–6801.
34 F. Long, H. Shi and H. Wang, *RSC Adv.*, 2014, **4**, 2935–2941.
35 L. Shi, Y. Jin and J. Liu, *Analyst*, 2024, **149**, 745–750.
36 Z. Guo, B. Yang, J. Zhu, S. Lou, H. Hao and W. Lu, *Food Chem.*, 2024, **436**, 137702.
37 Z. Guo, B. Yang, W. Lu, Z. Tian and H. Hao, *Anal. Chem.*, 2024, **96**, 3655–3661.
38 Y. Wang, J. Luo, J. Liu, X. Li, Z. Kong, H. Jin and X. Cai, *Biosens. Bioelectron.*, 2018, **107**, 47–53.
39 X. Zhang, Z. Shen, W. Su, H. Wu, S. C. B. Gopinath and R. Chen, *Process Biochem.*, 2020, **99**, 21–26.
40 Y. Matsumoto, H. Kuramitz, S. Itoh and S. Tanaka, *Talanta*, 2006, **69**, 663–668.